JOM, Vol. 67, No. 7, 2015
DOI: 10.1007/s11837-015-1342-7

A Method for Efficient Transmittance Spectrum Prediction of Transparent Composite Electrodes

ZHAO ZHAO,[1] A. DHAR,[2] and T. L. ALFORD[1,2,3]

1.—School for Engineering of Matter, and Energy, Arizona State University, Tempe, AZ 85287, USA. 2.—Department of Chemistry and Biochemistry, Arizona State University, Tempe, AZ 85287, USA. 3.—e-mail: TA@asu.edu

The interest in indium-free transparent composite electrode (TCE), a thin metal layer embedded between two transparent metal oxide (TMO) layers resulting in TMO/metal/TMO composite structure, has grown recently with the advent of their high figures of merit and its potential application in photovoltaic applications. However, most of the work to date has focused on experimentally producing the best optically transmitting TCE. To better design TCEs and minimize experimental work, it would be useful to develop a model that predicts the optical transmission. In the current work, the transfer-matrix method is employed to calculate the transmittance spectrum of TCE. To validate this approach, the transmittance spectra of TiO_2/Au/TiO_2 and TiO_2/Ag/TiO_2 multilayer thin-film TCEs are calculated with use of extracted material parameters. The calculated transmittance spectrum of TiO_2/Au/TiO_2 matches the measured spectrum quite well. However, the calcualted transmittance of TiO_2/Ag/TiO_2 is higher than its measured transmittance. The presence of voids in the Ag film is probably responsible for the decreased transmittance of the TiO_2/Ag/TiO_2 sample, and the continuous Au film in TiO_2/Au/TiO_2 ensures a good agreement between transmittance prediction and measurement. Our approach is a reliable tool to predict the optical transmittance of TCE with continuous films, and it can efficiently expedite the selection from numerous possible combinations of transparent metal oxides and metals when developing TCEs for future photovoltaic applications. It can also serve as a convenient method to assess the continuity of embedded metal layer.

INTRODUCTION

Indium tin oxide (ITO) electrodes have broad applications in solar cells, flat-panel displays, and organic emitting diodes.[1–4] However, ITO contains the rare-earth element indium, and the extensive use of ITO drives researchers to develop low cost and sustainable replacement for ITO electrodes.[1–4] In recent years, transparent composite electrodes (TCEs) attract much interest because of their competitive electrical and optical properties.[4,5] TCEs have a trilayer thin-film structure, in which a metal layer is embedded between two transparent metal oxide (TMO) layers.[1–12] TCE with the use of indium-free transparent oxide, such as TiO_2 and ZnO, not only has a lower cost than ITO but also can achieve a superior optical transmittance of 85% and low resistivity of 10^{-5} Ω cm.[4,5] As a composite structure, TMO and the embedded metal layers significantly affect the optical and electrical properties of TCEs.[11] To determine the desired TMO and metal layers to achieve high optical transmittance, TCEs are typically fabricated and tested by trial and error, but this method is costly and time consuming. An efficient prediction for the optical transmittance of TCE using material parameters is needed. In this study, the transfer-matrix method is used to calculate the transmittance of TCEs as a function of material parameters, including film thickness, refractive indices, and film roughness. To validate the approach, TiO_2/Au/TiO_2 and TiO_2/Ag/TiO_2 multilayer thin films are fabricated, and then their material parameters are extracted and incorporated into the transfer matrix to calculate the optical transmittance.

(Published online February 27, 2015)

MODEL

The transmittance of a subject can be calculated by taking the ratio of transmitted light intensity and incident light intensity.[13] However, multiple reflections within one layer have to be considered when light propagates in a multilayer structure.[13–15] All the transmitted waves resulting from multiple reflections within one layer have to be summed up and sequentially used as incident waves for the next layer.[13–15] To simplify the calculation, the transfer-matrix method has been adapted in the transmittance and reflectance calculation of multilayer thin-film structures.[16–18]

Light consists of an electric field component and a magnetic component. In the transfer-matrix method, all the waves propagating in the same direction at the same side of the interface are represented by one electric field. The forward electric fields at right side of layer i and the backward electric field at left side of the layer i+1 is represented by E_i^{fr} and E_{i+1}^{bl}, respectively. Figure 1 is the schematic of the simplified electric fields in trilayer TCE on a glass substrate. When conducting the transfer-matrix method, the layer whose thickness is comparable with the wavelength of light is treated as a coherent layer, and the layer with a thickness larger than the wavelength of light is considered as an incoherent layer.[17,18] Hence, our TCE model consisting of thin TMO and metal layers and a thick glass layer is a mixture of coherent and incoherent layers. In the transfer-matrix method, electric field amplitudes in coherent layers are correlated via matrix operation, and the light intensity, instead of field amplitudes, has to be employed when correlating waves in the incoherent layer.[16–18] Therefore, the coherent layers and incoherent layer have to be calculated separately in our model.

When a normal incident light propagates at the interface of coherent layer i and i+1, the electric fields at two sides of that interface could be correlated using transfer matrix $P_{i,i+1}$:

$$\begin{pmatrix} E_i^{\mathrm{fr}} \\ E_i^{\mathrm{br}} \end{pmatrix} = \frac{1}{t_{i,i+1}} \begin{pmatrix} 1 & r_{i,i+1} \\ r_{i,i+1} & 1 \end{pmatrix} \begin{pmatrix} E_{i+1}^{\mathrm{fl}} \\ E_{i+1}^{\mathrm{bl}} \end{pmatrix} = P_{i,i+1} \begin{pmatrix} E_{i+1}^{\mathrm{fl}} \\ E_{i+1}^{\mathrm{bl}} \end{pmatrix} \tag{1}$$

where $t_{i,i+1}$ and $r_{i,i+1}$ is the Fresnel transmission and reflection coefficients, respectively. They can be calculated using refractive indices of layer i and layer i+1. In terms of waves propagating within layer i+1, the electric field within layer i+1 can be correlated via transfer matrix P_{i+1}:

$$\begin{pmatrix} E_{i+1}^{\mathrm{fl}} \\ E_{i+1}^{\mathrm{bl}} \end{pmatrix} = \begin{pmatrix} e^{-i\delta_{i+1}} & 0 \\ 0 & e^{i\delta_{i+1}} \end{pmatrix} \begin{pmatrix} E_{i+1}^{\mathrm{fr}} \\ E_{i+1}^{\mathrm{br}} \end{pmatrix} = P_{i+1} \begin{pmatrix} E_{i+1}^{\mathrm{fr}} \\ E_{i+1}^{\mathrm{br}} \end{pmatrix} \tag{2}$$

where $\delta_{i+1}=2n_{i+1}d_{i+1}/\lambda$ is the phase change when the wave travels through layer i+1. n is the real part of the refractive index, d is the layer thickness, and λ is the wavelength. Within the coherent layers, the

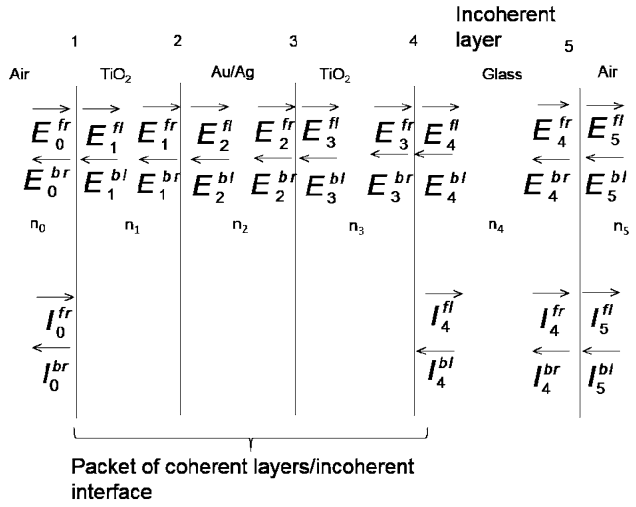

Fig. 1. Schematic of electric field amplitudes and light intensity within a TCE on glass.

incident electric fields at surface 1 and the transmitted electric fields coming from TiO_2 layer 3 can be correlated by multiplying the transfer matrices $P_{i,i+1}$ for each interface and P_{i+1} for each layer:

$$\begin{aligned} \begin{pmatrix} E_0^{\mathrm{fr}} \\ E_0^{\mathrm{br}} \end{pmatrix} &= P_{01}P_1P_{12}P_2P_{23}P_3P_{34} \begin{pmatrix} E_4^{\mathrm{fl}} \\ E_4^{\mathrm{bl}} \end{pmatrix} \\ &= P_{04} \begin{pmatrix} E_4^{\mathrm{fl}} \\ E_4^{\mathrm{bl}} \end{pmatrix} = \begin{pmatrix} M_{11} & M_{12} \\ M_{21} & M_{22} \end{pmatrix} \begin{pmatrix} E_4^{\mathrm{fl}} \\ E_4^{\mathrm{bl}} \end{pmatrix} \end{aligned} \tag{3}$$

where P_{04} is the transfer matrix for the packet of coherent layers and M_{ij} is the element in P_{04}. The transmittance and reflection coefficients for the packet of coherent layers are calculated using the elements in P_{04}:

$$t_{04} = \left.\frac{E_4^{\mathrm{fl}}}{E_0^{\mathrm{fr}}}\right|_{E_4^{\mathrm{bl}}=0} = \frac{1}{M_{11}} \tag{4a}$$

$$r_{04} = \left.\frac{E_0^{\mathrm{br}}}{E_0^{\mathrm{fr}}}\right|_{E_4^{\mathrm{bl}}=0} = \frac{M_{21}}{M_{11}} \tag{4b}$$

$$t_{40} = \left.\frac{E_0^{\mathrm{br}}}{E_4^{\mathrm{bl}}}\right|_{E_0^{\mathrm{fr}}=0} = \frac{Det\,M}{M_{11}} \tag{4c}$$

$$r_{40} = \left.\frac{E_4^{\mathrm{fl}}}{E_4^{\mathrm{bl}}}\right|_{E_0^{\mathrm{fr}}=0} = -\frac{M_{12}}{M_{11}} \tag{4d}$$

When waves reach the incoherent glass layer, the previous packet of coherent layers should be consid-

ered as an incoherent interface.[18] The light intensity at the incoherent interface and within incoherent glass layer is correlated using an incoherent transfer matrix.[17,18] The incoherent transfer matrix can be obtained by replacing the transmission and reflection coefficients in the coherent transfer matrix with their squared amplitudes.[17,18] The incoherent transfer matrices for the incoherent interface (packet of coherent layers) and for the incoherent glass layer are P_{04}^{incoh} and P_{4}^{incoh}, respectively:

$$P_{04}^{\text{incoh}} = \frac{1}{|t_{04}|^2}\begin{pmatrix} 1 & -|r_{40}|^2 \\ |r_{04}|^2 & |t_{04}t_{40}|^2 - |r_{04}r_{40}|^2 \end{pmatrix} \quad (5)$$

$$P_{4}^{\text{incoh}} = \begin{pmatrix} |e^{-i\delta_4}|^2 & 0 \\ 0 & |e^{i\delta_4}|^2 \end{pmatrix} \quad (6)$$

The incident light intensity and the light intensity coming from the glass substrate are correlated by:

$$\begin{pmatrix} I_0^{\text{fr}} \\ I_0^{\text{br}} \end{pmatrix} = P_{04}^{\text{incoh}} P_{4}^{\text{incoh}} P_{45}^{\text{incoh}} \begin{pmatrix} I_5^{\text{fl}} \\ I_5^{\text{bl}} \end{pmatrix} = M^{\text{incoh}} \begin{pmatrix} I_5^{\text{fl}} \\ I_5^{\text{bl}} \end{pmatrix} = \begin{pmatrix} M_{11}^{\text{incoh}} & M_{12}^{\text{incoh}} \\ M_{21}^{\text{incoh}} & M_{22}^{\text{incoh}} \end{pmatrix} \begin{pmatrix} I_5^{\text{fl}} \\ I_5^{\text{bl}} \end{pmatrix} \quad (7)$$

Hence, the transmittance of TCE can be expressed by:

$$T_{05} = \frac{I_5^{\text{fl}}}{I_0^{\text{fr}}} = \frac{1}{M_{11}^{\text{incoh}}} = |t_{04}|^2 \frac{|t_{45}|^2}{1 - |r_{40}r_{04}|^2} \quad (8)$$

It is noticeable that the rough interfaces will result in light scattering and decreased transmittance.[18–20] The transmission and reflection coefficients should be modified by multiplying the scattering factors to account for the scattering effect.[18–20] The scattering factor s^{r} for reflection and s^{t} for transmission are shown below:

$$s_{i-1,i}^{t} = \exp\left[-\frac{1}{2}\left(\frac{2\pi(n_{i-1} - n_i)\sigma_i}{\lambda}\right)^2\right] \quad (9)$$

$$s_{i-1,i}^{r} = \exp\left[-\frac{1}{2}\left(\frac{4\pi n_{i-1}\sigma_i}{\lambda}\right)^2\right] \quad (10)$$

where σ_i is the rms roughness of interface i.

Equation 8, which represents the transmittance of TCE, is a function of the refractive indices, thickness, and roughness of each single layer. Refractive indices of bulk materials and thin films are quite different, and different deposition techniques can result in different refractive indices of the thin films.[21] To ensure a reliable prediction, the material parameters used in the calculation have to be realistically represent properties of each layer. Hence, the extraction of optical indices is done on thin films that are deposited by the same technique and conditions used for the deposition of TCE.

EXPERIMENTAL

To validate our approach, TiO_2/Au/TiO_2 and TiO_2/Ag/TiO_2 multilayer thin-film TCEs were fabricated and their optical transmittance was measured. The trilayer structure, TiO_2/Au/TiO_2 and TiO_2/Ag/TiO_2, were sequentially deposited at room temperature onto glass substrates, respectively. The TiO_2 layer of TiO_2/Au/TiO_2 and TiO_2 layer of TiO_2/Ag/TiO_2 were deposited by rf sputtering TiO_2 target (99% purity) using different target-to-substrate distance with a power of 150 W under a pressure of 20 mTorr in Ar gas ambient. The metal layer was deposited onto the TiO_2 layer by dc sputtering Ag or Au target (99% purity) using the power of 40 W at the pressure of 10 mTorr in Ar gas ambient. The thickness of each layer was controlled by deposition time. To study the morphology of the midmetal layer, another set of two-layer structures, Ag/TiO_2 and Au/TiO_2, were deposited on glass using the corresponding deposition condition of their TCEs.

The optical transmittance of TCEs on glass at wavelength of 300 to 800 nm was measured by a double-channel spectrometer using air as a reference. The thickness of TiO_2 and Au thin films and the optical indices of TiO_2, Au, and Ag thin films were obtained by the variable angle spectroscopic ellipsometry and WVASE 32 software. The Ag thickness was acquired by Rutherford backscattering spectrometry and RUMP software. The roughness values of the surface and each interface in TCEs were determined by atomic force microscopy analysis in tapping mode. Because the glass substrate was very smooth, its roughness was considered as 0 nm. The thickness of each layer and the roughness of each interface in TCEs are listed in Table I. The morphology of Ag and Au layer was inspected by XL 30 environmental field emission secondary electron microscopy (SEM) using samples of Ag/TiO_2 and Au/TiO_2 on glass.

RESULT AND DISCUSSION

The transmittance spectra of TiO_2/Au/TiO_2 and TiO_2/Ag/TiO_2 on glass are predicted by the incorporation of the experimentally extracted material parameters into the transfer matrices. The calculated and experimentally measured transmittance spectra of TiO_2/Au/TiO_2/glass are shown in Fig. 2a. The calculation result shows a good agreement with the measurement result; therefore, our approach is demonstrated to be able to successfully predict the optical transmittance of TiO_2/Au/TiO_2 on glass.

Table I. Thickness and Roughness from TiO_2/Au/TiO_2 and TiO_2/Ag/TiO_2 Multilayer Thin-Film Structure

	Thickness (nm)				RMS Roughness (nm)		
	Layer 1 (TiO_2)	Layer 2 (Au/Ag)	Layer 3 (TiO_2)	Layer 4 (glass)	Surface 1	Interface 2	Interface 3
TiO_2/Au/TiO_2	38.4	10.5	39.7	10^6	1.746	0.680	0.766
TiO_2/Ag/TiO_2	30	12	30	10^6	1.817	1.187	0.852

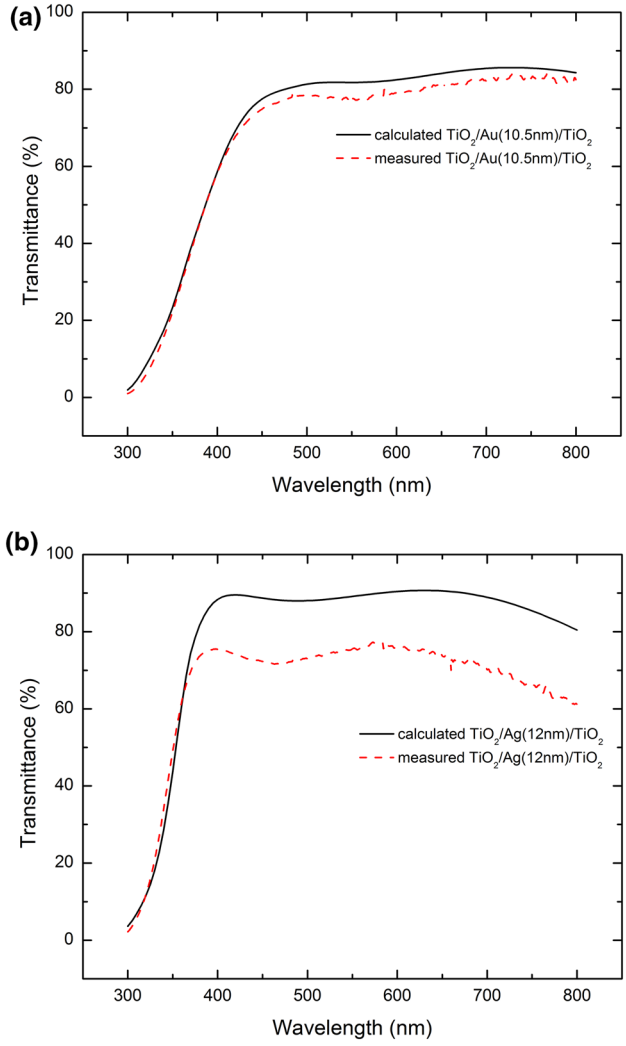

Fig. 2. Measured and calculated optical transmittance spectra from (a) TiO_2/Au/TiO_2 and (b) TiO_2/Ag/TiO_2 multilayer thin-film on glass substrate in wavelength range of 300 nm to 800 nm.

Figure 2b shows calculated transmittance spectrum of the TiO_2/Ag/TiO_2/glass and the spectrum measured from the TiO_2/Ag/TiO_2/glass sample. The calculated transmittance is higher than that measured from the TiO_2/Ag/TiO_2/glass sample. It might be due to the extra light absorption caused by discontinuous Ag film in TCE.[22]

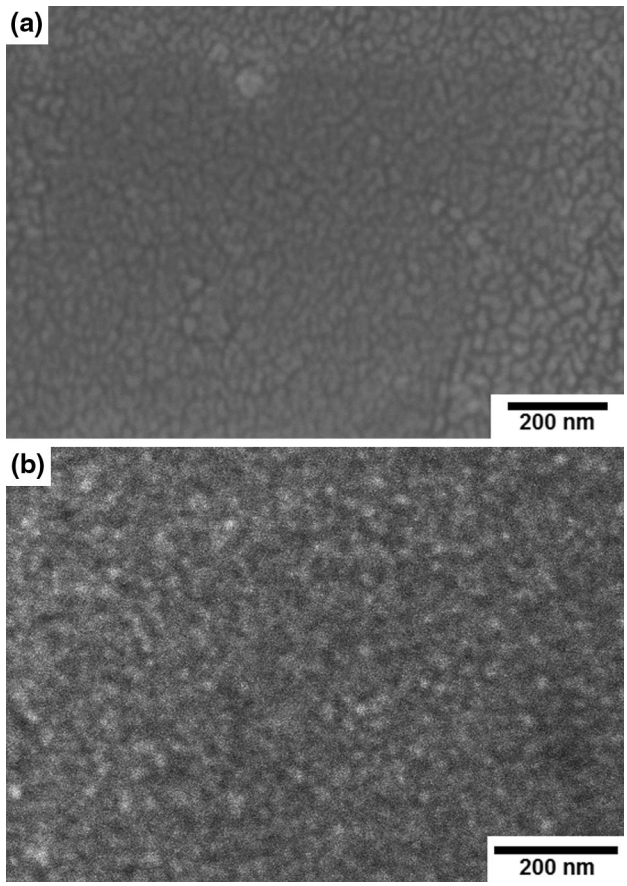

Fig. 3. SEM images from the surface of (a) Ag (12 nm)/TiO_2 on glass and (b) Au (10.5 nm)/TiO_2 on glass.

It has been reported that the voids in island-like Ag metal layer of TCE will result in decreased transmittance and increased absorption compared with TCE with continuous Ag thin film.[22] The SEM image of 12-nm Ag thin film sputtered on TiO_2 films in Fig. 3a indicates that the Ag thin film is not continuous yet. In our approach, all films are assumed to be continuous and the light absorption caused by voids in the films is not incorporated into the calculation because its mechanism is not clear yet. Hence, the predicted transmittance, which does not take account of voids in the actual Ag film, shows an optical transmittance higher than that measured from the TiO_2/Ag/TiO_2 sample. Compared

with $TiO_2/Ag/TiO_2$, the SEM image of 10.5-nm Au thin film on TiO_2 shows a continuous but rough Au layer in Fig. 3b. Therefore, the predicted transmittance of the corresponding $TiO_2/Au/TiO_2$ does not show deviation from the experimental transmittance.

The decreased transmittance of $TiO_2/Ag/TiO_2$ due to the discontinuous Ag layer implies that light absorption due to voids could be eliminated and high transmittance would be achieved by fabricating thin and continuous metal thin film in TCE.

CONCLUSION

The transfer-matrix method for mixed coherent and incoherent layers is utilized to calculate the transmittance of $TiO_2/Ag/TiO_2$ and $TiO_2/Au/TiO_2$ multilayer structure TCEs. The physical parameters (optical indices, thickness, and roughness) of each layer are extracted from the samples by means of ellipsometry, Rutherford backscattering spectrometry, and atomic force microscopy, and then they are incorporated into the calculation to ensure an accurate prediction. Our model assumes all layers are continuous. As a result, the $TiO_2/Au/TiO_2$, which proposes a continuous Au layer, shows a good agreement between its predicted and measured transmittance spectra. However, the predicted transmittance of $TiO_2/Ag/TiO_2$ is higher than its measured transmittance. This deviation is the result of the light absorption caused by voids in the discontinuous Ag film in $TiO_2/Ag/TiO_2$. It turns out that our approach is an efficient tool to predict the transmittance of TCEs with continuous thin film layer. It could assist in selecting the optimal materials from numerous candidates without fabricating all the recipes when designing high transmittance TCE. On the other hand, our approach could be used as an indicator for discontinuous layer if the calculated and measured transmittance does not match.

ACKNOWLEDGEMENTS

This work was partially supported by National Science Foundation (C. Ying, Grant No. DMR-0902277) to whom the authors are greatly indebted.

REFERENCES

1. K. Sivaramakrishnan and T.L. Alford, *Appl. Phys. Lett.* 96, 2011109 (2010).
2. A. Dhar and T.L. Alford, *APL Mater.* 1, 012102 (2013).
3. A. Dhar and T.L. Alford, *J. Appl. Phys.* 112, 103113 (2012).
4. A. Kumar, R. Srivastave, M.N. Kamalasanan, and D.S. Mehta, *Opt. Lett.* 37, 575 (2013).
5. J.H. Lee, K.Y. Woo, K.H. Kim, H.D. Kim, and T.G. Kim, *Opt. Lett.* 38, 5055 (2013).
6. C. Guillén and J. Herrero, *Thin Solid Films* 520, 1 (2011).
7. L. Cattin, M. Morsli, F. Dahou, S.Y. Abe, A. Khelil, and J.C. Bernède, *Thin Solid Films* 518, 4560 (2010).
8. D.R. Sahu, S.-Y. Lin, and J.-L. Huang, *Appl. Surf. Sci.* 252, 7509 (2006).
9. C. Guillén and J. Herrero, *Phys. Status Solidi A* 206A, 1531 (2009).
10. A. Dhar and T.L. Alford, *MRS Proc.* 1577, mrss11-1322-b06-04 (2013).
11. J.A. Jeong, Y.S. Park, and H.K. Kim, *J. Appl. Phys.* 107, 023111 (2010).
12. A. Dhar and T.L. Alford, *ECS Solid State Lett.* 3, N33 (2014).
13. E. Hecht and A. Zajac, *Optics* (Reading, MA: Addison-Wesley, 1974), pp. 71–88, 301–306.
14. P. Lecaruyer, E. Maillart, M. Canva, and J. Rolland, *Appl. Opt.* 45, 8419 (2006).
15. W. Ewart, *Applications of Interferometry* (London: Methuen, 1950), pp. 76–78.
16. Z.B. Wang, M.G. Helander, X.F. Xu, D.P. Puzzo, J. Qiu, M.T. Greiner, and Z.H. Lu, *J. Appl. Phys.* 109, 053107 (2011).
17. C.C. Katsidis and D.I. Siapkas, *Appl. Opt.* 41, 3978 (2002).
18. E. Centurioni, *Appl. Opt.* 44, 7532 (2005).
19. A. Poruba, A. Fejfar, Z. Remes, J. Springer, M. Vanecek, J. Kocka, J. Meier, P. Torres, and A. Shah, *J. Appl. Phys.* 88, 148 (2000).
20. P. Beckmann and A. Spizzichino, *The Scattering of Electromagnetic Waves from Rough Surfaces* (New York: Pergamon Press, 1963), pp. 80–91.
21. M.N. Polyanskiy, "Refractive index database," http://refractiveindex.info.
22. Y.C. Han, M.S. Lim, J.H. Park, and K.C. Choi, *IEEE Electron Device Lett.* 35, 238 (2014).